scientific reports

Check for updates

OPEN

On the yield criterion of porous materials by the homogenization approach and Steigmann–Ogden surface model

Chenyi Zheng✉, Hongzhen Wang, Yali Jiang & Gaohui Li✉

In this work, we investigate the yield criterion of nanoporous materials by using homogenization approach and Steigmann–Ogden surface model. The representative volume element is proposed as an infinite matrix containing a tiny nanovoid. The matrix is incompressible, rigid-perfectly plastic, von Mises materials and nanovoids are dilute and equal in size. First, the constitutive of microscopic stress and microscopic strain rate is established based on the flow criterion. Secondly, according to the Hill's lemma, the relationship between the macroscopic equivalent modulus and the microscopic equivalent modulus is established by homogenization approach. Thirdly, the macroscopic equivalent modulus containing the Steigmann–Ogden surface model including surface parameters, porosity and nanovoid radius is derived from the trial microscopic velocity field. Finally, an implicit macroscopic yield criterion for nanoporous materials is developed. For surface modulus, nanovoids radius and porosity studies are developed through extensive numerical experiments. The research results in this paper have reference significance for the design and manufacture of nanoporous materials.

Nanoporous materials have outstanding material properties, including high porosity[1], large specific surface area, high thermal conductivity, high electrical conductivity, high energy adsorption and corrosion resistance. Due to the superior properties of nanoporous materials, related research articles have also been developed, including the study of effective modulus[2,3], elastic response[4–7] and strength analysis of nanoporous materials[8,9].

Among these studies, most of the literature is limited to the effect of surface and interface mechanical responses on elastic properties, while lack of focus on strength criteria for nanoporous materials, which has important implications for the design and fabrication of nanoporous materials. In terms of the yield criterion of porous materials, Gurson[1] proposed the famous Gurson yield criterion based on the trial microscopic velocity field from the perspective of energy. The effect of void ratio on the macroscopic yield criterion is fully considered in the Gurson yield criterion, so that the macroscopic yield criterion depends on both the macroscopic equivalent stress and the macroscopic average stress. Since the effects of void interactions and coalescence were ignored, Tvergaard[10] improved the Gurson yield criterion by calibrating using finite element unit cell calculations. Tvergaard and Needleman[11] further extended the macroscopic yield criterion according to a set of elastic-plastic constitutive relations, known as the famous GTN model.

For the research on the yield criterion of nanoporous materials, scholars mainly carry out two methods: numerical and theoretical[12,13]. As an important numerical method, finite element theory is also used in the study of the yield criterion of nanoporous materials. Nasir et al.[14] combined a Gurson-type yield function including void size effects with finite element theory to predict the forming limit of aluminum materials based on the interfacial stress of the membrane around spherical voids. The results show that a smaller void size leads to an increase in the ductility limit of the material. Espeseth et al.[15] presented a numerical study of a finite element-based unit cell consisting of a single spherical void embedded in a matrix material, with size effects represented by a porous plastic model with voids. Espeseth investigated the effect of the intrinsic length scale of the matrix material on void growth and coalescence under a range of stress states. Unlike classical finite element theory, Usman et al.[16] investigated the effect of void shape on the micromechanisms of void growth by using discrete dislocation plasticity simulations and using the extended finite element method (XFEM) to model displacement discontinuities.

Huadong Engineering Corporation Limited, Hangzhou 311122, Zhejiang, China. ✉email: zheng_cy1@hdec.com; 594040623@qq.com

In the theoretical study of nanoporous materials, a typical method is to couple the strain gradient theory on the Gurson model. By combining strain gradient theory and the classical Gurson model, Li et al.[17] proposed a macroscopic yield criterion for spherical representative volume elements (RVEs) for axisymmetric tensile traction. Monchiet et al.[18] extends Gurson's yield criterion based on strain gradient theory and derives an approximate closed-form macroscopic yield function. On the basis of the strain gradient theory, the research on the yield criterion of nanoporous materials under complex working conditions is further developed. Niordson and Tvergaard[19] recently generalized the theory of strain gradient plasticity with dissipative gradient effects to finite strain in order to quantify the size-scale effect on void growth under different loading conditions. Ban[20] considers the influence of deformation damage on the basis of strain gradient plasticity theory and proposed a modified incremental constitutive model to characterize the coupling effect of size and damage in micro-metallic materials.

In addition to strain gradient theory, coupling surface theory at the interface of representative volume element (RVE) is also a recent popular practice. Based on the traditional Gurson model, Dormieux and Kondo[21] coupled the Gurtin-Murdoch surface model at the inner surface of the spherical void to deduce the macroscopic yield function of nanoporous materials and explored the effect of surface parameters on the macroscopic yield loci. Monchiet[22] used the same method to study the macroscopic yield function of nanoporous materials with viscoplastic matrix. Next, Monchiet and Kondo[23] further studied the yield criterion of nanoporous materials under ellipsoidal RVE. However, the Gurtin-Murdoch surface model only considers the surface tensile stress, while ignoring the existence of the surface compressive stress[24,25]. In order to supplement this deficiency, Zheng and Mi[13] obtained the macroscopic yield criterion of nanoporous materials based on the Steigmann–Ogden surface model and explored the mechanism of surface bending moment.

Different from the Gurson model, the homogenization approach establishes the macroscopic yield function of nanoporous materials from the perspective of energy, which depends on the relationship between the macroscopic equivalent modulus and the matrix modulus. Due to the existence of critical points of elasticity and plasticity, scholars can derive the macroscopic yield function of nanoporous materials from the perspectives of elastic limit and plastic flow. Zhang et al.[26] derived the macroscopic yield function of nanoporous materials considering the Gurtin-Murdoch surface model from the perspective of elastic limit and studied the influence of surface elastic parameters on the macroscopic yield function. Chen[27] used the same method to study the macroscopic yield function of nanoporous materials with columnar RVE. Zheng and Mi[28] combined the homogenization theory and the Gurson model to derive the macroscopic yield function of multi-scale nanoporous materials.

Besides the analysis of elastic limit, Dormieux and Kondo[8] firstly derived the macroscopic yield function of nanoporous materials from the perspective of plastic flow, in which the imperfect interface is replaced by a thin film. In order to solve the problem of plastic modulus, Brach et al.[29] based on the layered method solved the equivalent plastic modulus under different layers of matrix and deduced the macroscopic yield criterion of nanoporous materials, respectively. Subsequently,[30] further studied the macroscopic yield function of nanoporous materials with general matrix under axisymmetric conditions. However, the above analysis ignores the influence of surface compressive stress on the imperfect interface.

The purpose of this paper is to continue the previous work, consider the influence of surface compressive stress on imperfect interface from the perspective of plastic flow and obtain the macroscopic yield criterion of nanoporous materials. Firstly, based on the plastic flow criterion, the plastic constitutive of the von Mises matrix is studied. Secondly, through the homogenization approach, the equivalent shear modulus of the matrix is obtained. Thirdly, according to the law of conservation of energy, the relationship between the macroscopic equivalent modulus and the microscopic equivalent modulus is derived. Finally, the macroscopic yield criterion of the nanoporous material considering the Steigmann–Ogden surface model is obtained through the trial velocity field.

The remainder of this paper is structured as follows. Section 2 details the homogenization approach and the derivation of the macroscopic equivalent modulus containing Steigmann–Ogden surface model. According to the Hill's lemma, the macroscopic yield criterion of nanoporous materials is obtained. In Section 3, extensive parametric studies are conducted in order to examine the effects of nanovoids surface bulk modulus, shear modulus, bending rigidity, nanovoids radius and porosity on the yield loci of nanoporous materials. In Section 4, concluding remarks are made.

Method of solution

Figure 1 shows the nanoporous materials containing multiple nanovoids inside. All multiple nanovoids are assumed to share the same radius and be far apart but to distribute randomly in space. To intercept a nanovoid as representative volume element (RVE), a standard Mori-Tanaka model will be considered, which is completely consistent with the image on the right side of Figure 1. a and b are denoted as the inner and outer radii of the RVE, respectively. Among them, the magnitude of the outer radius is much larger than the inner radius ($a \gg b$) . The volumes occupied by the void, matrix and RVE are denoted by V_1, V_2 and V_3, respectively. The outer boundary of the RVE is subjected to an arbitrary axisymmetric macroscopic strain rate ($\mathbf{D}$).

Homogenization approach. Let us consider that the matrix of the RVE satisfies the von Mises yield criterion. The yield surface of the matrix is denoted by $g(\sigma)$:

$$g(\sigma) = \frac{3}{2}\sigma_d : \sigma_d - \sigma_Y^2 \leq 0, \tag{1}$$

where σ_d and σ_Y stand for the microscopic deviatoric stress and microscopic yield stress for the whole RVE. By means of the plastic flow criterion, the microscopic strain rate can be easily obtained:

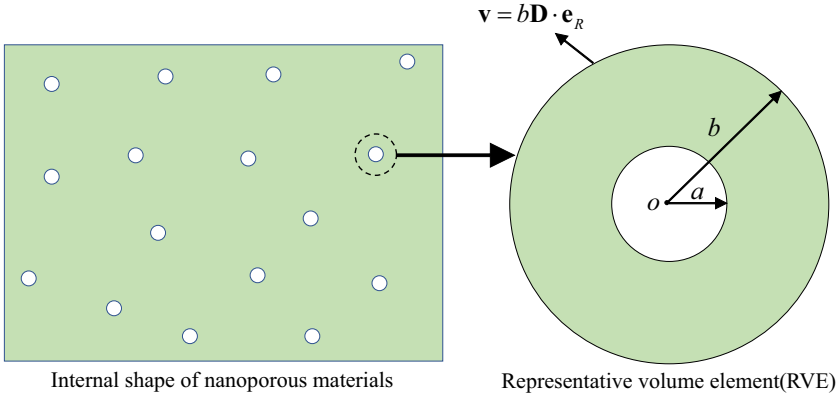

Figure 1. The nanoporous materials containing spherical nanovoids and the representative volume element (RVE).

$$\mathbf{d} = \dot{\lambda}\frac{\partial f(\sigma)}{\partial \sigma} = 3\dot{\lambda}\sigma_d, \tag{2}$$

where $\dot{\lambda}$ denotes plastic flow rate. For the convenience of subsequent derivation, the fourth-order mean projection tensor $\mathbb{J}$ and the deviatoric projection tensor $\mathbb{K}$ can be introduced here. Their tensor form can be represented by index notation:

$$J_{ijkl} = \frac{1}{3}\delta_{ij}\delta_{kl}, \quad K_{ijkl} = I_{ijkl} - J_{ijkl}, \quad I_{ijkl} = \frac{1}{2}\left(\delta_{ik}\delta_{jl} + \delta_{il}\delta_{jk}\right), \tag{3a-c}$$

where δ_{ij} and I_{ijkl} indicate identity second-order tensor and identity fourth-order tensor. Using the projection tensor, Equation (2) can be easily simplified to

$$\mathbf{d} = 3\dot{\lambda}\mathbb{K} : \sigma. \tag{4}$$

Simultaneously multiplying the deviatoric projection tensor on both sides of the Equation (4):

$$\mathbb{K} : \mathbf{d} = 3\dot{\lambda}\mathbb{K} : \mathbb{K} : \sigma. \tag{5}$$

It is not difficult to obtain the expression of the microscopic deviatoric stress by the fourth-order deviatoric projection tensor:

$$\sigma_d = \mathbb{K} : \sigma = \frac{1}{3\dot{\lambda}}\mathbb{K} : \mathbf{d}. \tag{6}$$

Substituting Eq. (6) into the yield function (1) of the matrix in limit state, the plastic flow rate ($\dot{\lambda}$) can be derived

$$\dot{\lambda} = \frac{1}{\sigma_Y}\sqrt{\frac{1}{6}\mathbf{d}' : \mathbf{d}'}, \tag{7}$$

where $\mathbf{d}'$ denotes the microscopic deviatoric strain rate. Knowing the form of microscopic stress and microscopic strain rate, the maximum plastic dissipation at any point in the RVE matrix can be expressed as

$$\pi(\mathbf{d}) = \sigma : \mathbf{d} = \sigma_Y d_{eq}. \tag{8}$$

Here, we exploit the principle of plastic dissipation consistency to solve for the equivalent strain rate (d_{eq}) at the limit state

$$d_{eq} = \sqrt{\frac{2}{3}\mathbf{d}' : \mathbf{d}'}. \tag{9}$$

The plastic constitutive equation of the microscopic stress can be derived by the plastic flow criterion

$$\sigma = \frac{\partial \pi(\mathbf{d})}{\partial \mathbf{d}} = \frac{2}{3}\frac{\sigma_Y}{d_{eq}}\mathbf{d}', \tag{10}$$

where $\pi(\mathbf{d})$ denotes the yield function of the matrix in terms of microscopic strain rate with the Equations (6, 7). Here we introduce the fourth-order plastic constitutive tensor ($\mathbb{C}_2$) of the matrix to support the following derivation

$$\sigma = \mathbb{C}_2 : \mathbf{d} = 2\mu_2{}'(\mathbf{d}')\mathbb{K} : \mathbf{d}. \tag{11}$$

Since the matrix is incompressible, the plastic constitutive of the microscopic stress can be simplified by the fourth-order deviatorial strain projection tensor. The shear modulus of plasticity $\mu_2{}'(\mathbf{d}')$ is a function of the microscopic deviatoric strain rate. By Equations (10, 11), it is not difficult to obtain the functional expression of the plastic shear modulus

$$2\mu_2{}'(\mathbf{d}') = \frac{2}{3}\frac{\sigma_Y}{d_{eq}(\mathbf{d}')}. \tag{12}$$

The non-constant nature of the plastic shear modulus can greatly increase the difficulty of solving the dissipation. To solve this puzzle,[8] proposed microscopic equivalent modulus shear modulus by homogenization approach

$$2\mu_2 = \frac{2}{3}\frac{\sigma_Y}{\tilde{d}_{eq}}. \tag{13}$$

where μ_2 is the average plastic shear modulus. We introduce a reference deviatoric strain rate, defined as

$$\tilde{d}_{eq} = \sqrt{\frac{2}{3}\overline{\mathbf{d}' : \mathbf{d}'}}. \tag{14}$$

The expression of the average operator is

$$\bar{\cdot} = \frac{1}{V}\int_V \cdot dV. \tag{15}$$

The Hill's lemma is presented

$$\Sigma : \mathbf{D} = (1-f)\overline{\sigma : \mathbf{d}}, \tag{16}$$

where the average operator here acts on the macroscopic representative volume of nanoporous materials, as shown in the left figure of Figure 1.

The plastic dissipation of the RVE from the macro perspective is expressed as

$$\Pi(\mathbf{D}) = \Sigma : \mathbf{D} = \mathbf{D} : (3\kappa_3\mathbb{J} + 2\mu_3\mathbb{K}) : \mathbf{D} = \Sigma : \left(\frac{1}{3\kappa_3}\mathbb{J} + \frac{1}{2\mu_3}\mathbb{K}\right) : \Sigma. \tag{17}$$

For macroscopic RVE, the equivalent bulk and shear plastic moduli are assumed to be constants and denoted as κ_3 and λ_3. Since the outer boundary of RVE is subjected to a uniform strain rate, the macroscopic strain rate is constant.

Combined with equations (13,14), the plastic dissipation of the RVE from a micro perspective is expressed as

$$\overline{\pi(\mathbf{d})} = \overline{\sigma : \mathbf{d}} = \overline{2\mu_2\mathbf{d} :\mathbb{K}: \mathbf{d}} = 2\mu_2\overline{\mathbf{d}' : \mathbf{d}'} = \frac{1}{3}\frac{\sigma_Y^2}{\mu_2}. \tag{18}$$

Combined with the Hill's lemma and energy perturbation (17,18), the relationship between the macroscopic strain rate and the microscopic strain rate at the minimum potential energy is established

$$\Sigma : \left(\frac{1}{3\delta\kappa_3}\mathbb{J} + \frac{1}{2\delta\mu_3}\mathbb{K}\right) : \Sigma = (1-f)\frac{\sigma_Y^2}{3\delta\mu_2}. \tag{19}$$

The macroscopic yield criterion can be further established

$$3\frac{\mu_2^2}{\kappa_3^2}\frac{\delta\kappa_3}{\delta\mu_2}\left(\frac{\Sigma_m}{\sigma_Y}\right)^2 + \frac{\mu_2^2}{\mu_3^2}\frac{\delta\mu_3}{\delta\mu_2}\left(\frac{\Sigma_{eq}}{\sigma_Y}\right)^2 - 1 + f = 0, \tag{20}$$

where

$$\Sigma_m = \frac{\mathrm{tr}(\Sigma)}{3}, \quad \Sigma_{eq} = \sqrt{\frac{3}{2}\Sigma' : \Sigma'}, \quad \Sigma' = \Sigma - \Sigma_m\mathbf{I}. \tag{21a-c}$$

From equation (20), it can be observed that the macroscopic yield criterion depends only on the porosity (f), the microscopic equivalent shear modulus (μ_2) and the macroscopic equivalent bulk and shear moduli (κ_3 and μ_3).

Macroscopic equivalent bulk modulus (κ_3). For any macroscopic strain rate, the strain rate field in the main direction can be obtained by coordinate transformation. As a basic form, only the axisymmetric case is considered in this paper. The macroscopic strain rate of the Cartesian coordinate system established in the principal direction is expressed as:

$$\mathbf{D} = \begin{bmatrix} D_m + D_e & 0 & 0 \\ 0 & D_m + D_e & 0 \\ 0 & 0 & D_m - 2D_e \end{bmatrix}, \tag{22}$$

where the macroscopic mean strain rate and the macroscopic deviatoric strain rate are denoted by D_m and D_e, respectively. Among them, the macroscopic equivalent bulk and shear moduli are generated only by the macroscopic mean strain rate and the macroscopic deviatoric strain rate, respectively.

Now, we will establish that the microscopic velocity field is generated only by the macroscopic mean strain rate:

$$v_R^1 = F_1 R + G_1 \frac{a^3}{R^2}, \quad v_\varphi^1 = v_\theta^1 = 0, \tag{23a,b}$$

$$v_R^2 = F_2 R + G_2 \frac{a^3}{R^2}, \quad v_\varphi^2 = v_\theta^2 = 0, \tag{23c,d}$$

where the superscripts 1 and 2 denote the inclusions and matrix of the microscopic RVE, respectively. The microscopic strain rate can be obtained by geometric equations

$$d_{ij}^1 = \frac{1}{2}\left(v_{i,j}^1 + v_{j,i}^1\right), \quad d_{ij}^2 = \frac{1}{2}\left(v_{i,j}^2 + v_{j,i}^2.\right) \tag{24a,b}$$

Establish the constitutive equation of microscopic stress

$$\sigma_{ij}^1 = \lambda_1 d_{kk}^1 \delta_{ij} + 2\mu_1 d_{ij}^1, \quad \sigma_{ij}^2 = \lambda_2 \varepsilon_{kk}^2 \delta_{ij} + 2\mu_2 d_{ij}^2, \tag{25a,b}$$

where $\lambda_{1,2} = \left(3\kappa_{1,2} - 2\mu_{1,2}\right)/3$.

There are four unknown coefficients on the microscopic velocity field that need to be determined by boundary conditions. The kinematic equations should be satisfied on the outer boundary.

$$v_R^2|_{R=b} = D_m b \tag{26}$$

Considering that the velocity field at the center of the sphere cannot be singular, the form of the unknown coefficient G_1 should be

$$G_1 = 0. \tag{27}$$

At the interface, the continuity condition of the velocity field should be guaranteed

$$v_R^1|_{R=a} = v_R^2|_{R=a}. \tag{28}$$

Steigmann-Ogden governing equations[5] for the force balance condition across a solid interface is described as

$$[\sigma] \cdot \mathbf{n} = \nabla_S \cdot \boldsymbol{\tau} + \nabla_S \cdot ((\nabla_S \cdot \mathbf{M})\mathbf{n}) - (\nabla_S \cdot \mathbf{n})\mathbf{n} \cdot (\nabla_S \cdot \mathbf{M})\mathbf{n}, \tag{29}$$

where ∇_S, $\boldsymbol{\tau}$, $\mathbf{M}$ and $\mathbf{n}$ denote the surface projection gradient in spherical coordinates, surface stress, surface bending moment and unit outer normal vector of the sphere, respectively. For the convenience of solving, the second-order surface projection tensor T_{ij} and normal projection tensor N_{ij} are introduced

$$T_{ij} = \delta_{ij} - n_i n_j, \quad N_{ij} = n_i n_j. \tag{30a,b}$$

It is easy to find that the surface projection tensor and the normal projection tensor are orthogonal and normal.

$$T_{ij} T_{jk} = T_{ik}, \quad T_{ij} N_{jk} = 0, \quad N_{ij} N_{jk} = N_{ik}. \tag{31a-c}$$

Split gradient operator into normal direction and surface direction

$$\frac{\partial}{\partial x_j} = N_{ij} \frac{\partial}{\partial x_i} + T_{ij} \frac{\partial}{\partial x_i}, \tag{32}$$

where surface gradient operator ∇_S is written as $T_{ij} \frac{\partial}{\partial x_i}$ in index notation. The surface bending moment is expressed as

$$M_{ij} = \zeta_s \kappa_{kk} T_{ij} + 2\chi_s \kappa_{ij}, \quad \kappa_{ij} = -\frac{1}{2}\left(\vartheta_{k,u} + \vartheta_{u,k}\right) T_{iu} T_{kj}, \quad \vartheta_i = T_{ij} n_k v_{k,j}. \tag{33a-c}$$

The surface stress is expressed as

$$\tau_{ij} = \lambda_0 d_{kk}^s \delta_{ij} + 2\mu_0 d_{ij}^s, \quad d_{ij}^s = T_{ik} d_{kl} T_{lj}. \tag{34a-b}$$

Through the above efforts, the interface stress condition (29) with surface effect can be rewritten as

$$[\sigma]_{ij} n_i = \tau_{ij,i} + T_{lu}\left(M_{kl,k} n_j\right)_{,u} - T_{ik} n_{i,k} n_l M_{ml,m} n_j \tag{35}$$

By calculation, it can be obtained

$$T_{ik}n_{i,k} = \frac{2}{a}. \tag{36}$$

The surface stress condition of the Steigmann-Ogden model can be further rewritten as

$$[\sigma]_{ij}n_i = \tau_{ij,i} + T_{lu}\left(M_{kl,k}n_j\right)_{,u} - \frac{2}{a}M_{ml,m}n_jn_l. \tag{37}$$

Using the trial velocity field, the slope change vector ϑ_i is written as

$$\vartheta_i = T_{ij}n_kv_{k,j} = 0. \tag{38}$$

From this, it can be judged that the surface bending moment does not participate under the action of the macroscopic mean strain rate due to $M_{ij} = 0$. Therefore, the surface stress condition of Steigmann-Ogden surface model will degenerate into the surface stress condition of Gurtin-Murdoch surface model.

$$[\sigma]_{ij}n_i = \tau_{ij,i} \tag{39}$$

Through the above four boundary conditions (26, 27, 28, 39), the four unknown coefficients (F_1, F_2, G_1, G_2) contained in the microscopic velocity field can be uniquely determined.

Define the average microscopic strain rate as[2]:

$$\bar{d}_{ij} = \frac{1}{2V}\int_S \left(n_iv_j + n_jv_i\right)dS. \tag{40}$$

The average strain rate of the matrix and the average strain rate of the inclusions are expressed as

$$\bar{d}^2_{ij} = \frac{1}{2V_2}\int_S \left(n_iv^2_j + n_jv^2_i\right)dS = D_m\delta_{ij}, \tag{41a}$$

$$\bar{d}^1_{ij} = \frac{1}{2V_1}\int_S \left(n_iv^1_j + n_jv^1_i\right)dS = \frac{D_m(3\kappa_2 + 4\mu_2)}{3\kappa_1 + 2(2+\kappa_s)\mu_2}\delta_{ij}, \tag{41b}$$

where

$$\kappa_s = \frac{\kappa_0}{a\mu_2}, \quad \mu_s = \frac{\mu_0}{a\mu_2}, \quad \eta_s = \frac{\eta_0}{a^3\mu_2}, \quad \kappa_0 = 2(\mu_0 + \lambda_0), \quad \eta_0 = 3\zeta_s + 5\chi_s. \tag{42a-e}$$

Then the microscopic equivalent strain rate and stress of the micro RVE are written as

$$\bar{d}^3_{ij} = (1-f)\bar{d}^2_{ij} + f\bar{d}^1_{ij}, \tag{43a}$$

$$\bar{\sigma}^3_{ij} = f\left(\bar{\sigma}^1_{ij} + \bar{\tau}_{ij}\right) + (1-f)\bar{\sigma}^2_{ij} = 3\kappa_3\bar{d}^3_{ij}, \tag{43b}$$

where

$$\bar{\tau}_{ij} = \frac{1}{V_1}\int_s [\sigma]_{ki}n_kx_jdA. \tag{44}$$

Combining equations (43,44), the macroscopic equivalent bulk modulus can be obtained

$$\kappa_3 = \frac{-3\kappa_1(3\kappa_2 + 4f\mu_2) - 2\mu_2\left(\kappa_2(6 - 6f + 3\kappa_s) + 4f\kappa_s\mu_2\right)}{9(-1+f)\kappa_1 - 6(2+\kappa_s)\mu_2 + f(-9\kappa_2 + 6\kappa_s\mu_2)}. \tag{45}$$

Considering that the inclusion is a nanovoid, its bulk modulus (κ_1) and shear modulus (μ_1) are both 0. Since the microscopic matrix is von Mises matrix, the microscopic bulk modulus is infinite. The macroscopic equivalent bulk modulus can be further simplified

$$\kappa_3 = \frac{2(2 - 2f + \kappa_s)\mu_2}{3f}. \tag{46}$$

Macroscopic equivalent shear modulus (μ_3). The macroscopic shear modulus is only affected by the macroscopic deviatoric strain rate:

$$\mathbf{D} = D_e\mathbf{e}_x\mathbf{e}_x + D_e\mathbf{e}_y\mathbf{e}_y - 2D_e\mathbf{e}_z\mathbf{e}_z. \tag{47}$$

To this end, the microscopic velocity field subjected only to the macroscopic deviatoric strain rate field is expressed as

$$v_R^1 = \left(F_{11}\frac{R^2}{a^2} + F_{12} + F_{13}\frac{a^3}{R^3} + F_{14}\frac{a^5}{R^5}\right) R P_2(\cos\varphi), \tag{48a}$$

$$v_\varphi^1 = \left(G_{11}\frac{R^2}{a^2} + G_{12} + G_{13}\frac{a^3}{R^3} + G_{14}\frac{a^5}{R^5}\right) R\partial_\varphi P_2(\cos\varphi), \tag{48b}$$

$$v_R^2 = \left(F_{21}\frac{R^2}{a^2} + F_{22} + F_{23}\frac{a^3}{R^3} + F_{24}\frac{a^5}{R^5}\right) R P_2(\cos\varphi), \tag{48c}$$

$$v_\varphi^2 = \left(G_{21}\frac{R^2}{a^2} + G_{22} + G_{23}\frac{a^3}{R^3} + G_{24}\frac{a^5}{R^5}\right) R\partial_\varphi P_2(\cos\varphi), \tag{48d}$$

$$v_\theta^1 = 0, \quad v_\theta^2 = 0, \tag{48e,f}$$

where $P_2(\cos\varphi)$ is the Legendre polynomial of order two.

Taking into account the geometric and constitutive equations (24a,b, 25a,b), substitute the microscopic stress into the stress balance equation:

$$\sigma_{ij,i}^1 = 0, \quad \sigma_{ij,i}^2 = 0. \tag{49a-b}$$

Based on equation (49a-b), eight unknown coefficients in the microscopic velocity field can be determined as

$$G_{11} = \frac{5F_{11}\lambda_1 + 7F_{11}\mu_1}{6\lambda_1}, \quad G_{12} = \frac{F_{12}}{2}, \tag{50a,b}$$

$$G_{13} = \frac{F_{13}\mu_1}{3\lambda_1 + 5\mu_1}, \quad G_{14} = -\frac{F_{14}}{3}, \tag{50c,d}$$

$$G_{21} = \frac{5F_{21}\lambda_2 + 7F_{21}\mu_2}{6\lambda_2}, \quad G_{22} = \frac{F_{22}}{2}, \tag{50e,f}$$

$$G_{23} = \frac{F_{23}\mu_2}{3\lambda_2 + 5\mu_2}, \quad G_{24} = -\frac{F_{24}}{3}. \tag{50g,h}$$

There are still 8 unknown coefficients in the microscopic velocity field that need to be determined by boundary conditions. First, the kinematic equations need to be satisfied on the boundary of the microscopic RVE.

$$v_R^2|_{R=b} = 2D_e b \tag{51}$$

By calculation, the form of the two coefficients can be determined

$$F_{21} = 0, \quad F_{22} = 2D_e. \tag{52a,b}$$

Second, the microscopic velocity field at the center of the microscopic RVE should avoid singularity, which requires that

$$F_{14} = 0, \quad F_{13} = 0. \tag{53a,b}$$

Third, the microscopic velocity field at the interface should satisfy the continuity condition:

$$v_R^1|_{R=a} = v_R^2|_{R=a}, \quad v_\varphi^1|_{R=a} = v_\varphi^2|_{R=a}. \tag{54a,b}$$

By solving equation (54a,b), two unknown coefficients can be obtained

$$F_{12} = -\frac{7(\lambda_1 + \mu_1)}{5\lambda_1}F_{11} + \frac{2}{5}\left(1 + \frac{3\mu_2}{3\lambda_2 + 5\mu_2}\right)F_{23} + 2D_e, \tag{55a}$$

$$F_{24} = -\frac{(2\lambda_1 + 7\mu_1)}{5\lambda_1}F_{11} - \frac{9(\lambda_2 + \mu_2)}{5(3\lambda_2 + 5\mu_2)}F_{23}. \tag{55b}$$

Finally, the stress condition containing the Steigmann–Ogden surface model needs to be satisfied at the interface.

$$[\sigma]_{ij}n_i = \tau_{ij,i} + T_{lu}\left(M_{kl,k}n_j\right)_{,u} - \frac{2}{a}M_{ml,m}n_j n_l \tag{56}$$

According to solving equation (56), the specific expressions of F_{11} and F_{23} can be finally obtained.

Given the definition of the microscopic strain rate equation (40), the microscopic average strain rate of the matrix and inclusions can be written as

$$\bar{d}_{ij}^{2} = -D_e \mathbf{e}_x \mathbf{e}_x - D_e \mathbf{e}_y \mathbf{e}_y + 2D_e \mathbf{e}_z \mathbf{e}_z, \tag{57a}$$

$$\bar{d}_{ij}^{1} = -D_b \mathbf{e}_x \mathbf{e}_x - D_b \mathbf{e}_y \mathbf{e}_y + 2D_b \mathbf{e}_z \mathbf{e}_z, \tag{57b}$$

$$D_b = \frac{5F_{12}\lambda_1 + 7F_{11}(\lambda_1 + \mu_1)}{10\lambda_1}. \tag{57c}$$

Based on the average microscopic strain rate, the average stress can be expressed as

$$\bar{d}_{ij}^{3} = (1-f)\bar{d}_{ij}^{2} + f\bar{d}_{ij}^{1}, \tag{58a}$$

$$\bar{\sigma}_{ij}^{3} = f\left(\bar{\sigma}_{ij}^{1} + \bar{\tau}_{ij}\right) + (1-f)\bar{\sigma}_{ij}^{2} = 2\mu_3 \bar{d}_{ij}^{3}, \tag{58b}$$

In terms of equations (57, 58, 42a-e), the macroscopic equivalent shear modulus can be easily derived

$$\mu_3 = \frac{2(l_3 + 2l_4) - 3f(l_1 + 2l_2)}{2(l_3 + 2l_4) + 2f(l_1 + 2l_2)}\mu_2, \tag{59}$$

where

$$l_1 = (2+\kappa_s)(1-\mu_s), \quad l_2 = \eta_s(1-\kappa_s - 3\mu_s), \tag{60a,b}$$

$$l_3 = 3 + 2\kappa_s + 3\mu_s + \kappa_s\mu_s, \quad l_4 = \eta_s(3 + \kappa_s + 3\mu_s). \tag{60c,d}$$

Finally, by substituting equations (59, 45) into equation (20), the macroscopic yield criterion of porous metals with Steigmann–Ogden surface model can be finally derived.

Results and discussion

In the previous section, we derived the yield criterion of porous materials by using homogenization approach and Steigmann–Ogden surface model. The yield criterion is analytical and implicit with respect to the macroscopic mean and equivalent stresses. The purpose of this section is to explore the effect of the parameters of the Steigmann–Ogden surface model, the radius of the nanovoid and the porosity on the macroscopic yield criterion. For the microscopic RVE, the matrix material is treated as aluminum with the shear modulus $\mu_2 = 23.6$ GPa and the yield strength $\sigma_Y = 250$ MPa. Following Tian's research[31], two sets of surface bulk modulus and shear modulus are considered for nanovoids surface: Case 1 ($\kappa_0 = 12.95$ nN/nm, $\mu_0 = -0.376$ nN/nm) and Case 2 ($\kappa_0 = -3.86$ nN/nm, $\mu_0 = -5.43$ nN/nm). For the surface bending moduli of nanovoids, which are additionally considered in the Steigmann–Ogden surface model, three surface parameters are taken into account ($\eta_0 = 0, -30, -60$ nN nm). For comparison, the classical solutions without considering the surface effects are also listed in the figure as much as possible.

Figure 2 shows the macroscopic yield loci of nanoporous aluminum at different surface bending moduli. The porosity and the nanovoid radius are taken as $f = 0.1$ and $a = 1$ nm. It can be clearly observed that Case 1 effectively increases the mean and equivalent stresses of the macroscopic yield loci, while Case 2 reduces the macroscopic mean and equivalent stresses. When the surface bending modulus (η_0) is taken as 0, the Steigmann–Ogden surface model degenerates to the Gurtin-Murdoch surface model. It can therefore be concluded from Fig. 2 that the surface bending modulus only affects the equivalent stress of the macroscopic yield loci, not the mean stress. The equivalent stress of the macroscopic yield loci is amplified regardless of the change in the surface bending modulus.

Figure 3 depicts the macroscopic yield loci of nanoporous aluminum at different nanovoid radii. The porosity and the surface bending moduli are taken as $f = 0.1$ and $\eta_0 = -30$nN nm, respectively. A phenomenon worth noting is that regardless of the value of the nanovoid radius, Case 1 enlarges the macroscopic yield loci of nanoporous aluminum, while case2 narrows the macroscopic yield loci. Regardless of Case 1 or Case 2, with the increase of the nanovoid radius, the surface effect will decay rapidly and approach the classical solution. Compared with Case 1, Case 2 can effectively change the mean stress of the macroscopic yield loci while the effect on the equivalent stress is very limited.

Figure 4 shows the macroscopic yield loci of nanoporous aluminum subjected to different porosity. The nanovoids radius and the surface bending modulus are taken as $a = 1$nm and $\eta_0 = -30$nN nm, respectively. It can be observed that when the porosity increases, the macroscopic yield loci shrink significantly. When the porosity is taken to be 0, the surface effect does not exist. And the macroscopic yield loci of nanoporous aluminum will degenerate into the von Mises yield loci. Another obvious phenomenon is that Case 1 significantly increases the equivalent stress of the macroscopic yield loci, while Case 2 has a very weak effect on the equivalent stress. As the porosity increases, the amplifying effect of Case 1 on the equivalent stress of the macroscopic yield loci is continuously enhanced.

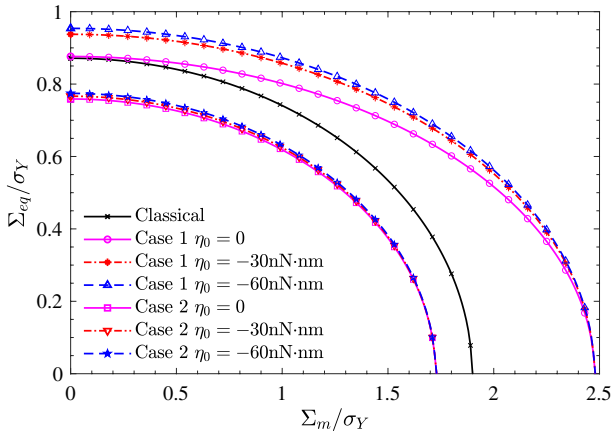

Figure 2. Effect of surface bending modulus (η_0) on the macroscopic yield loci of nanoporous aluminum. The porosity and the nanovoid radius are taken as $f = 0.1$ and $a = 1$ nm. Two sets of surface bulk and shear moduli are considered: Case 1 ($\kappa_0 = 12.95$ nN/nm, $\mu_0 = -0.376$ nN/nm) and Case 2 ($\kappa_0 = -3.86$ nN/nm, $\mu_0 = -5.43$ nN/nm).

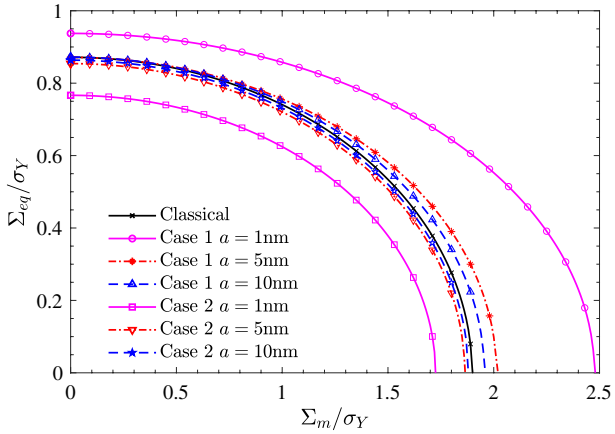

Figure 3. Effect of nanovoids radius (a) on the macroscopic yield loci of nanoporous aluminum. The porosity and the surface bending modulus are taken as $f = 0.1$ and $\eta_0 = -30$nN · nm. Two sets of surface bulk and shear moduli are considered: Case 1 ($\kappa_0 = 12.95$ nN/nm, $\mu_0 = -0.376$ nN/nm) and Case 2 ($\kappa_0 = -3.86$ nN/nm, $\mu_0 = -5.43$ nN/nm).

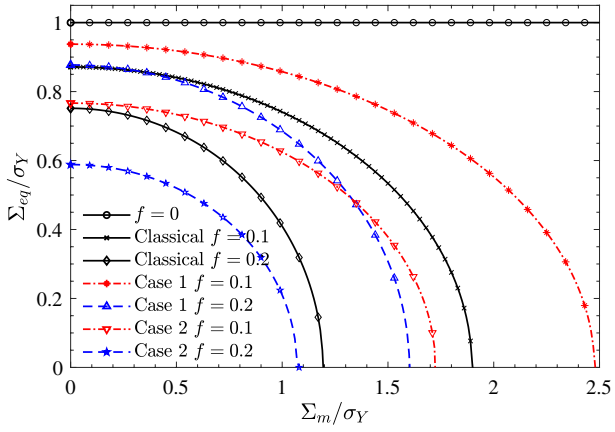

Figure 4. Effect of porosity (f) on the macroscopic yield loci of nanoporous aluminum. The nanovoids radius and the surface bending modulus are taken as $a = 1$nm and $\eta_0 = -30$nN nm. Two sets of surface bulk and shear moduli are considered: Case 1 ($\kappa_0 = 12.95$ nN/nm, $\mu_0 = -0.376$ nN/nm) and Case 2 ($\kappa_0 = -3.86$ nN/nm, $\mu_0 = -5.43$ nN/nm).

Concluding remarks

In this paper, we developed a macroscopic yield criterion for nanoporous materials based on the homogenization approach and Steigmannn–Ogden surface model. The RVE is described as the classic Mori-Tanaka model, that is, an infinite matrix containing a tiny nanaovoid. The surface effects of nanovoids are applied at the interface between the nanovoid and the matrix. Firstly, based on the homogenization approach, the macroscopic yield criterion of nanoporous materials is obtained, which includes the dependence of the macroscopic equivalent modulus and the microscopic uniform modulus. Secondly, based on the establishment of the trial velocity field, the macroscopic equivalent modulus including the influence of the Steigmannn–Ogden model can be obtained. Finally, an implicit macroscopic yield criterion for nanoporous materials is derived. Based on the surface modulus, porosity and nanopore radius, related studies were developed and analyzed in detail. On the basis of extensive parametric studies, a few major conclusions can be drawn as follows.

- Different surface moduli will have different regulation effects on the macroscopic yield criterion of nanoporous materials. Positive surface moduli significantly increase the macroscopic yield loci, while negative surface moduli decrease the macroscopic yield loci slightly.
- The surface bending modulus only affects the equivalent stress of the macroscopic yield loci and has no effect on the mean stress.
- The influence of surface effects on the macroscopic yield criterion of nanoporous materials strongly depends on the size of the nanovoid radius. The smaller the radius of the nanopore, the more obvious the surface effect.
- The macroscopic yield criterion of nanoporous materials strongly depends on the size of the porosity. The larger the macroscopic porosity, the more obvious the shrinkage of the macroscopic yield loci.

Data availability

The datasets used and analysed during the current study available from the corresponding author on reasonable request.

Received: 18 February 2023; Accepted: 2 July 2023
Published online: 06 July 2023

References

1. Gurson, A. L. Continuum theory of ductile rupture by void nucleation and growth: Part I—yield criteria and flow rules for porous ductile media. *J. Eng. Mater. Technol.* **99**(1), 2–15. https://doi.org/10.1115/1.3443401 (1977).
2. Duan, H., Wang, J., Huang, Z. & Karihaloo, B. Size-dependent effective elastic constants of solids containing nano-inhomogeneities with interface stress. *J. Mech. Phys. Solids* **53**(7), 1574–1596. https://doi.org/10.1016/j.jmps.2005.02.009 (2005).
3. Duan, H., Yi, X., Huang, Z. & Wang, J. A unified scheme for prediction of effective moduli of multiphase composites with interface effects part i: Theoretical framework. *Mech Mater.* **39**(1), 81–93. https://doi.org/10.1016/j.mechmat.2006.02.009 (2007).
4. Ban, Y. & Mi, C. Analytical solutions of a spherical nanoinhomogeneity under far-field unidirectional loading based on Steigmann-Ogden surface model. *Math. Mech. Solids* **25**(10), 1904–1923. https://doi.org/10.1177/1081286520915259 (2020).
5. Ban, Y. & Mi, C. On spherical nanoinhomogeneity embedded in a half-space analyzed with Steigmann-Ogden surface and interface models. *Int. J. Solids Struct.* **216**, 123–135. https://doi.org/10.1016/j.ijsolstr.2020.11.034 (2021).
6. Mi, C. & Kouris, D. Stress concentration around a nanovoid near the surface of an elastic half-space. *Int. J. Solids Struct.* **50**(18), 2737–2748. https://doi.org/10.1016/j.ijsolstr.2013.04.029 (2013).
7. Zemlyanova, A. Y. & Mogilevskaya, S. G. Circular inhomogeneity with Steigmann-Ogden interface: Local fields, neutrality, and Maxwell's type approximation formula. *Int. J. Solids Struct.* **135**, 85–98. https://doi.org/10.1016/j.ijsolstr.2017.11.012 (2018).
8. Dormieux, L. & Kondo, D. Non linear homogenization approach of strength of nanoporous materials with interface effects. *Int. J. Eng. Sci.* **71**, 102–110. https://doi.org/10.1016/j.ijengsci.2013.04.006 (2013).
9. Monchiet, V., Charkaluk, E. & Kondo, D. Macroscopic yield criteria for ductile materials containing spheroidal voids: An Eshelby-like velocity fields approach. *Mech. Mater.* **72**, 1–18. https://doi.org/10.1016/j.mechmat.2013.05.006 (2014).
10. Tvergaard, V. Influence of voids on shear band instabilities under plane strain conditions. *Int. J. Fract.* **17**(4), 389–407. https://doi.org/10.1007/bf00036191 (1981).
11. Tvergaard, V. & Needleman, A. Analysis of the cup-cone fracture in a round tensile bar. *Acta Metall.* **32**(1), 157–169. https://doi.org/10.1016/0001-6160(84)90213-x (1984).
12. Wen, J., Huang, Y., Wang, K. H., Liu, C. & Li, M. The modified Gurson model accounting for the void size effect. *Int. J. Plast.* **21**(2), 381–395. https://doi.org/10.1016/j.ijplas.2004.01.004 (2005).
13. Zheng, C., Zhang, G. & Mi, C. On the strength of nanoporous materials with the account of surface effects. *Int. J. Eng. Sci.* **160**, 103451. https://doi.org/10.1016/j.ijengsci.2020.103451 (2021).
14. Nasir, M. W., Chalal, H. & Abed-Meraim, F. Prediction of forming limits for porous materials using void-size dependent model and bifurcation approach. *Meccanica* **55**(9), 1829–1845. https://doi.org/10.1007/s11012-020-01222-1 (2020).
15. Espeseth, V., Morin, D., Faleskog, J., Børvik, T. & Hopperstad, O. S. A numerical study of a size-dependent finite-element based unit cell with primary and secondary voids. *J. Mech. Phys. Solids* **157**, 104493. https://doi.org/10.1016/j.jmps.2021.104493 (2021).
16. Usman, M., Waheed, S. & Mubashar, A. Effect of shape on void growth: A coupled extended finite element method (XFEM) and discrete dislocation plasticity (DDP) study. *Eur. J. Mech. A/Solids* **92**, 104471. https://doi.org/10.1016/j.euromechsol.2021.104471 (2022).
17. Li, Z., Huang, M. & Wang, C. Scale-dependent plasticity potential of porous materials and void growth. *Int. J. Solids Struct.* **40**(15), 3935–3954. https://doi.org/10.1016/s0020-7683(03)00178-1 (2003).
18. Monchiet, V. & Bonnet, G. A Gurson-type model accounting for void size effects. *Int. J. Solids Struct.* **50**(2), 320–327. https://doi.org/10.1016/j.ijsolstr.2012.09.005 (2013).
19. Niordson, C. F. & Tvergaard, V. A homogenized model for size-effects in porous metals. *J. Mech. Phys. Solids* **123**, 222–233. https://doi.org/10.1016/j.jmps.2018.09.004 (2019).
20. Ban, H., Peng, Z., Fang, D., Yao, Y. & Chen, S. A modified conventional theory of mechanism-based strain gradient plasticity considering both size and damage effects. *Int. J. Solids Struct.* **202**, 384–397. https://doi.org/10.1016/j.ijsolstr.2020.05.023 (2020).

21. Dormieux, L. & Kondo, D. An extension of Gurson model incorporating interface stresses effects. *Int. J. Eng. Sci.* **48**(6), 575–581. https://doi.org/10.1016/j.ijengsci.2010.01.004 (2010).
22. Monchiet, V. & Bonnet, G. Interfacial models in viscoplastic composites materials. *Int. J. Eng. Sci.* **48**(12), 1762–1768. https://doi.org/10.1016/j.ijengsci.2010.09.024 (2010).
23. Monchiet, V. & Kondo, D. Combined voids size and shape effects on the macroscopic criterion of ductile nanoporous materials. *Int. J. Plast.* **43**, 20–41. https://doi.org/10.1016/j.ijplas.2012.10.007 (2013).
24. Steigmann, D. J. & Ogden, R. W. Plane deformations of elastic solids with intrinsic boundary elasticity. *Proc. Royal Soc. London Ser. A Math. Phys. Eng. Sci.* **453**, 853–877. https://doi.org/10.1098/rspa.1997.0047 (1997).
25. Steigmann, D. J. & Ogden, R. W. Elastic surface-substrate interactions. *Proc. Royal Soc. London Ser. A Math. Phys. Eng. Sci.* **455**(1982), 437–474. https://doi.org/10.1098/rspa.1999.0320 (1999).
26. Zhang, W. X. & Wang, T. J. Effect of surface energy on the yield strength of nanoporous materials. *Appl. Phys. Lett.* **90**(6), 063104. https://doi.org/10.1063/1.2459115 (2007).
27. Chen, H., Liu, X. & Hu, G. Overall plasticity of micropolar composites with interface effect. *Mech. Mater.* **40**(9), 721–728. https://doi.org/10.1016/j.mechmat.2008.03.005 (2008).
28. Zheng, C. & Mi, C. On the macroscopic strength criterion of ductile nanoporous materials. *Int. J. Eng. Sci.* **162**, 103475. https://doi.org/10.1016/j.ijengsci.2021.103475 (2021).
29. Brach, S., Dormieux, L., Kondo, D. & Vairo, G. Strength properties of nanoporous materials: A 3-layered based non-linear homogenization approach with interface effects. *Int. J. Eng. Sci.* **115**, 28–42. https://doi.org/10.1016/j.ijengsci.2017.03.001 (2017).
30. Brach, S., Anoukou, K., Kondo, D. & Vairo, G. Limit analysis and homogenization of nanoporous materials with a general isotropic plastic matrix. *Int. J. Plast.* **105**, 24–61. https://doi.org/10.1016/j.ijplas.2017.10.007 (2018).
31. Tian, L. & Rajapakse, R. Finite element modelling of nanoscale inhomogeneities in an elastic matrix. *Comput. Mater. Sci.* **41**(1), 44–53. https://doi.org/10.1016/j.commatsci.2007.02.013 (2007).

Acknowledgements

This work was supported by the Innovation Project of Huadong Engineering Corporation Limited [Grant Numbers KY2023-SD-02-02].

Author contribution

Both authors materially participated in the research and preparation of this manuscript. H.W. and Y.J. conceived, designed and composed the research. C.Z. and G.L. conducted the analytical derivation of the yield function and the velocity field and also performed the parametric analysis.Both authors approved the final version of the manuscript and its submission.

Competing interests

The authors declare no competing interests.

Additional information

Correspondence and requests for materials should be addressed to C.Z. or G.L.

Reprints and permissions information is available at www.nature.com/reprints.

Publisher's note Springer Nature remains neutral with regard to jurisdictional claims in published maps and institutional affiliations.